

Assessment of Lead-Bismuth Eutectic Target Material for Accelerator Driven Transmuters

Yousry Gohar

Argonne National Laboratory
9700 South Cass Avenue
Argonne, IL 60439, USA
gohar@anl.gov

Abstract

Lead-Bismuth Eutectic is under consideration as a target material with high-energy protons for generating spallation neutrons to operate actinide and fission product transmuters. An assessment has been performed to study the performance of this target material as a function of the main variables and the design selections. The assessment includes the neutron yield, the spatial energy deposition, the neutron spectrum, the beam window performance, and the target buffer requirements. Heat transfer, hydraulics, beam window material and stresses, and target engineering issues have been considered. The assessment has also considered high-energy deuteron particles to study the impact on the target performance.

Introduction

Lead-Bismuth Eutectic (LBE) technology is being developed worldwide for spallation neutron targets, which will drive subcritical transmuters. This paper is intended to assess the LBE material performance including the impact of the main variables and the design selections. The charged particle energy, the target buffer thickness, the charged particle type, and the window material selection are considered in the assessment. The performance analysis includes the neutron yield, the neutron utilization fraction, the neutron spatial distribution, the neutron spectrum, the energy deposition per neutron, the beam window nuclear responses, the window operating life, and the nuclear responses in the structural material outside the target buffer. The analysis was performed for proton and deuteron charged particles to compare the impact on the LBE material performance. In the analysis process, heat transfer, hydraulics, beam window stresses, and target engineering issues have been considered to insure that the obtained performance is achievable for the LBE target designs.

The MCNPX code [1] was used to perform the physics analysis. The engineering analysis utilized different computer codes to satisfy the different design rules and criteria [2]. The assessment results are given in the paper as well as the main conclusion from the analysis. The paper defines the design parameter values to operate the LBE material in spallation targets with a satisfactory performance. Also, recommendations

are obtained to maximize the neutron utilization and protect the structural material outside the target buffer from the charged particles and the high-energy neutrons.

Energy Deposition

The first step in the analysis was to define the energy deposition profile in the LBE for different proton energies. MCNPX computer code was used for this function with proton energy in the range of 200 to 1000 MeV. The results are shown in Figure 1, which are normalized to the neutron current density. The peak energy deposition does not occur at the LBE surface but it is inside the LBE material along the beam axis. Such behavior is desirable because the beam window will not be exposed to the peak heating value. Also, it does simplify the LBE heat removal. Increasing the charged particle energy reduces the peak power density and spreads the energy deposition in the lead-bismuth. As the proton energy increases above 600 MeV, the peak value shifts from the end of proton beam range to the beam entry area, at about 1 cm from the surface.

The total energy deposition increases linearly as the proton energy increases. However, the energy loss percentage to the endothermic reactions increases as the proton energy increases. The energy deposition per generated neutron shows a very fast decrease with the proton energy up to about 500 MeV, and then it slows down as shown in Figure 2. Such behavior encourages the use of high-energy proton to reduce the target cooling requirements for specific neutron source strength.

Neutron Yield

The number of neutrons per proton increases as the proton energy increases up to 500 MeV and then it increases linearly as shown in Figure 3. However, the neutron fraction with energy above 20 MeV reaches a saturation value of ~ 0.05 as the proton energy increases, as shown in Figure 3. The neutron utilization fraction is defined as the neutron fraction of the total generated neutrons that does not leave the target volume in the beam direction because these neutrons have the opportunity to perform material transmutation. The neutrons leaving the target volume in the beam direction will interact with the shield, the reflector, or the transmuter structural material. The neutron utilization fraction changes from 0.53 at 200 MeV to 0.81 at 1000 MeV proton energy. As the proton energy increases, the neutrons are generated further away from the LBE surface, which increases the radial neutron leakage and subsequently the neutron utilization factor. The neutron distribution in the different directions (Top, Radial, and Bottom) is shown in Figure 4. In this analysis, an adequate target length is included to slow down, multiply, and reflect the high-energy neutrons at the end of the proton range (referred to as the bottom section). This enhances the neutron production per proton and the neutron utilization fraction. Also, a fixed buffer thickness of 7 cm is used in the analyses to protect the structural material outside the target and it can serve as a coolant manifolds. The effect of the buffer thickness on the neutron utilization fraction is discussed later. Again, these results shows that the use of high-energy proton is beneficial for enhancing the neutron yield as well as the neutron utilization factor.

Neutron Source Spatial Distribution

In the transmuter design, axial power peaking is a design issue, which has a significant impact on the transmuter performance. The spatial neutron source distribution has a direct impact on the power peaking in the driven systems. It is desirable to distribute uniformly the neutron source in the axial direction to reduce the power peaking. The spatial neutron source distribution was calculated at the outer surface of the 7-cm buffer for different proton energies as shown in Figure 5 per neutron source. The results show that the neutron source distribution uniformity in the beam direction improves as the proton energy increases. The neutron peak is reduced by a factor of two as the proton energy increases from 200 to 1000 MeV. Also, the neutron peak is shifted further by about 8 cm along the beam direction and the neutron spatial distribution spreads further along the beam axis. These results show that the use of high-energy proton help reducing the axial power peaking in the driven transmuters.

Neutron Source Spectrum

The neutron source spectra at the outer buffer surface for different proton energies are shown in Figure 6. The small wiggles in the neutron spectrum between 0.045 and 0.075 MeV are due to the LBE resonance cross sections in this energy range. The neutron spectra are very similar up to 80 MeV. Above the 80 MeV, the neutron density is reduced by a factor in the range of 10^4 to 10^8 relative to the peak value at 0.55 MeV. The average neutron energy is about 1 MeV compared to 2 MeV for the fission spectrum. Figure 7 shows both the neutron source spectrum and the fission spectrum. The neutron source spectrum is softer than the fission spectrum however it has a very high-energy tail as shown in Figure 6. This high-energy tail affects the nuclear responses in the structure material. It enhances the helium production rate, which affects the mechanical properties of the structural materials; further details are given in the buffer size section.

Beam Window Nuclear Responses

As an example, the nuclear responses in the beam window are given in Table 1 for the 600 MeV protons and the beam current is normalized to $40 \mu\text{A}/\text{cm}^2$. The energy deposition density in the HT-9 beam window is $766.5 \text{ W}/\text{cm}^3$ and the peak value in the LBE material is $796 \text{ W}/\text{cm}^3$ at 1.75 cm from the LBE surface. In the beam window, the neutrons are responsible for 69% of the atomic displacement and the protons are generating more than 96% of the gas production rate. The high gas production rate affects the mechanical properties of the window material, which requires experimental data for realistic lifetime prediction of the structural material. Current structural analysis [2] utilizing experimental fission data with lower helium per atomic displacement shows that the beam window may be able to operate for full power year with a current density of $40 \mu\text{A}/\text{cm}^2$.

Buffer Requirement and Impact on the Neutron Utilization

The analysis was performed as a function of the buffer thickness with MCNPX. The cross section areas required for the inlet and the outlet manifolds define the minimum buffer thickness, which is 7 cm for 5 MW Beam with 600 MeV protons [2]. The neutron yield (number of neutrons per proton) has a low sensitivity to the buffer thickness as shown in Figure 8. The neutron yield reaches a saturation value at a buffer thickness of ~40 cm. The saturation value is about 1.14 times the value obtained with the 7-cm minimum buffer thickness. However, the number of neutrons utilized for material transmutation is significantly reduced as the buffer thickness is increased. This is also shown in Figure 8 where the neutron utilization fraction drops from 0.71 with 7-cm buffer to 0.25 with 40-cm buffer. The axial neutron leakage is increased as the buffer thickness is increased. This requires the target design to reduce the buffer thickness as much as possible.

The nuclear responses in the structural material at the outer buffer surface of a fast transmuter system change linearly with the reciprocal of the outer buffer radius [2]. The other important parameter for the structural material performance is the helium to atomic displacement ratio. Figure 9 shows this ratio as a function of the buffer thickness for HT-9 alloy, which is in the range of 0.1 to 0.3. This ratio is about 0.26 for HT-9 in a typical fast reactor spectrum. For the above beam parameters with a fast transmuter, the results show that the 7-cm buffer thickness protects the structural material from the nuclear responses caused by the high energy neutrons ($E > 20$ MeV), utilizes most of the generated neutrons, and has adequate cross section area for the inlet and the outlet LBE coolant manifolds. Therefore, the lifetime of the structural material around the buffer will depend on the operating temperature, the nuclear response, and the loading conditions similar to fast fission systems.

Deuterons versus Protons for Neutron Generation

Another assessment for the LBE material performance was performed with deuterons instead of the protons. The deuteron energy was varied in the range of 200 to 1000 MeV similar to the proton assessment. The energy deposition profile in the LBE for different deuteron energies is shown in Figure 10 and the results are normalized to the neutron current density. The deuteron energy deposition profiles are similar to the proton profiles. However the range of the deuterons with Energy E is about twice the range of the proton with energy $E/2$. Also, the peak energy deposition from the deuterons is about twice the corresponding value for the proton with same energy. This means that the neutrons are generated over shorter range, which have positive impact the transmutation neutrons as will be discussed later.

Similar to the proton case, the total energy deposition and the neutron production increase as the deuteron energy increases. The Deuteron generates slightly more energy than the proton of the same energy and more neutrons. In the energy range of 400 to 1000 MeV, the deuteron generates about 7 to 9% more neutrons relative to the proton with the same energy. The deuteron has a shorter range where the spallation

neutrons are generated. The forward high-energy spallation neutrons have a better chance for neutron multiplication through (n,xn) reactions with LBE. The resulting neutron spectrum is slightly softer because of this effect and spreads over the same range similar to the proton case. Figure 11 shows neutron source distribution along the target buffer outer surface for different proton and deuteron energies, which show the deuteron generates more neutrons than the proton with similar spatial distribution.

Conclusions

The LBE assessment of this paper reached the following main conclusions:

1. Increasing the charged particle energy reduces the peak power density and spreads the energy deposition in the lead-bismuth. Such effects reduce the maximum window temperature and facilitate the heat removal process from the target.
2. The energy deposition per generated neutron decreases fast as the charged particle energy increases up to ~600 MeV, then it decreases slowly.
3. The neutron yield increases with the energy of the charged particles. However the high-energy neutron ($E > 20$ MeV) fraction reaches a saturation value of about 5% of the total generated neutrons as the charged particle energy increases.
4. The neutron uniformity increases in the beam direction as the energy of the charged particles increases. The peak value is always shifted away from the lead-bismuth surface. Increasing the source uniformity reduces the power peaking in the transmuter.
5. The high-energy neutrons ($E > 20$ MeV) have similar spatial distribution with more shifting for the peak value in the beam direction away from the beam entry surface.
6. The generated neutron spectrum does not change with the energy of the charged particles except for the upper end of the spectrum, which is 4 to 8 order of magnitude less than the peak value.
7. The average spallation neutron energy is ~1 MeV compared to 2 MeV for fission neutron spectrum. However, the high-energy tail of the spallation neutrons affects the nuclear responses in the structural materials.
8. The use of lead-bismuth buffer with a small thickness, which is required for the inlet and outlet coolant manifolds, reduces the nuclear responses in the structural material around the target to the observed values in the fast fission reactors.
9. The neutron balance analysis shows that the large buffer thickness reduces significantly the neutron utilization factor. For example, at 40-cm buffer thickness, the neutron utilization factor is 0.25, which means a beam power loss of 75%.
10. The range of the deuteron with Energy E is about twice the range of the proton with energy $E/2$. Also, the peak energy deposition from the deuteron is about twice the corresponding value for the proton with same energy.
11. In lead-bismuth, deuterons produce slightly more neutrons than protons. For the same axial target length and shorter deuteron range, the high-energy spallation neutrons produce more (n,xn) reactions with LBE, which increase the neutron production per deuteron. The difference is about 7 to 9 % for the deuterons in the energy range of 400 to 1000 MeV.

Acknowledgements

The submitted manuscript has been created by the University of Chicago as Operator of Argonne National Laboratory ("Argonne") under contract No. W-31-109-ENG-38 with the U.S. Department of Energy. The U.S. Government retains for itself, and others acting on its behalf, a paid-up, nonexclusive, irrevocable worldwide license in said article to reproduce, prepare derivative works, distribute copies to the public, and perform publicly and display publicly, by or on behalf of the Government.

References

1. MCNPX Team, "MCNPX Version 2.4.j," Los Alamos National Laboratory, LA-UR-02-2127 (25 March, 2002)
2. Yousry Gohar, Phillip J. Finck, et. Al., "Lead- Bismuth Target Design for the Subcritical Multiplier (SCM) of the Accelerator Driven Test Facility (ADTF)," Argonne National Laboratory Report, ANL/TD/02-01, 2002.

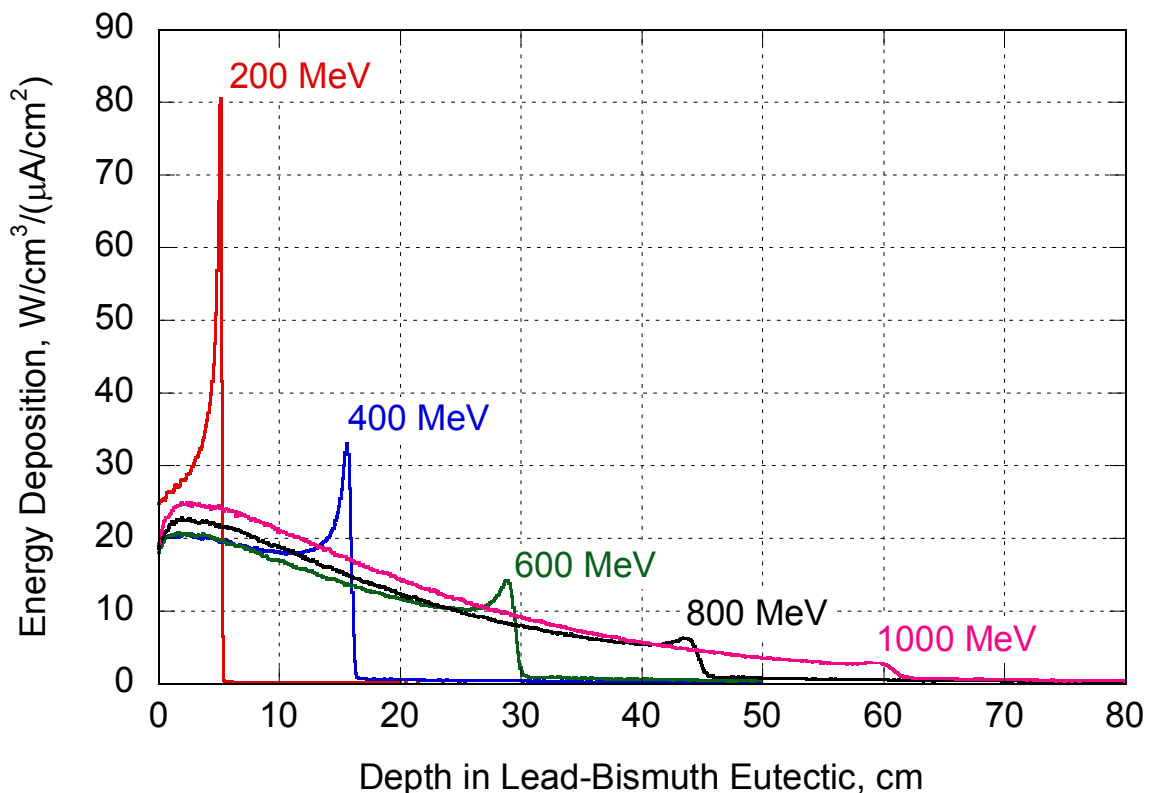


Figure 1. Spatial energy deposition in the lead-bismuth eutectic for different proton energies

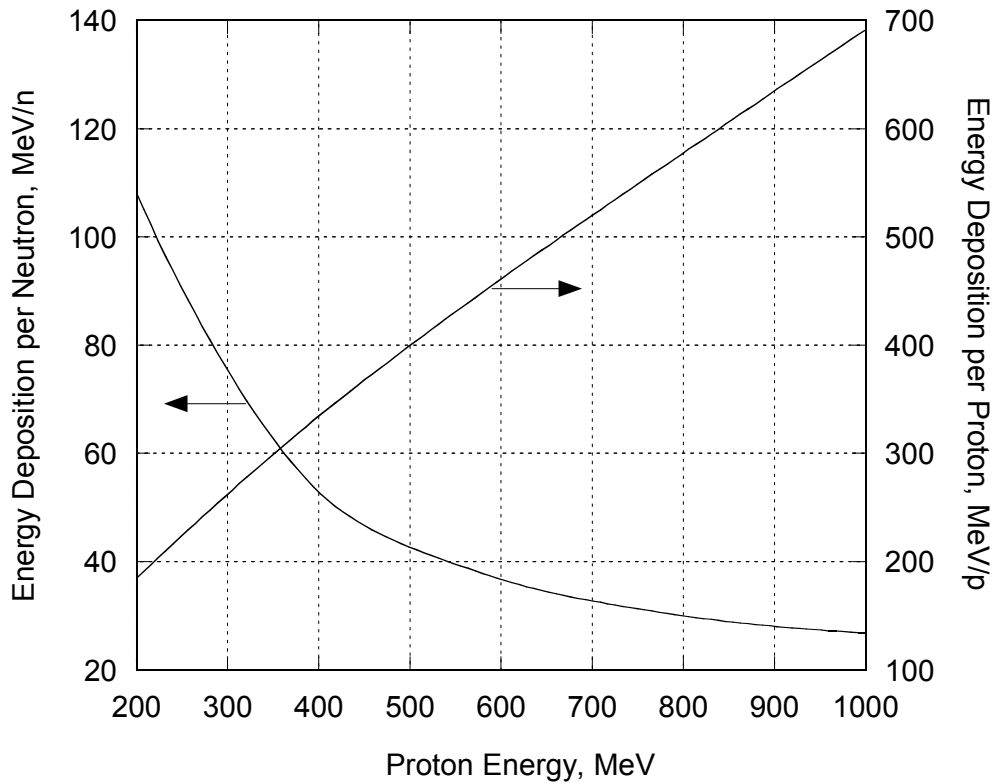


Figure 2. Energy deposition as a function of the proton energy

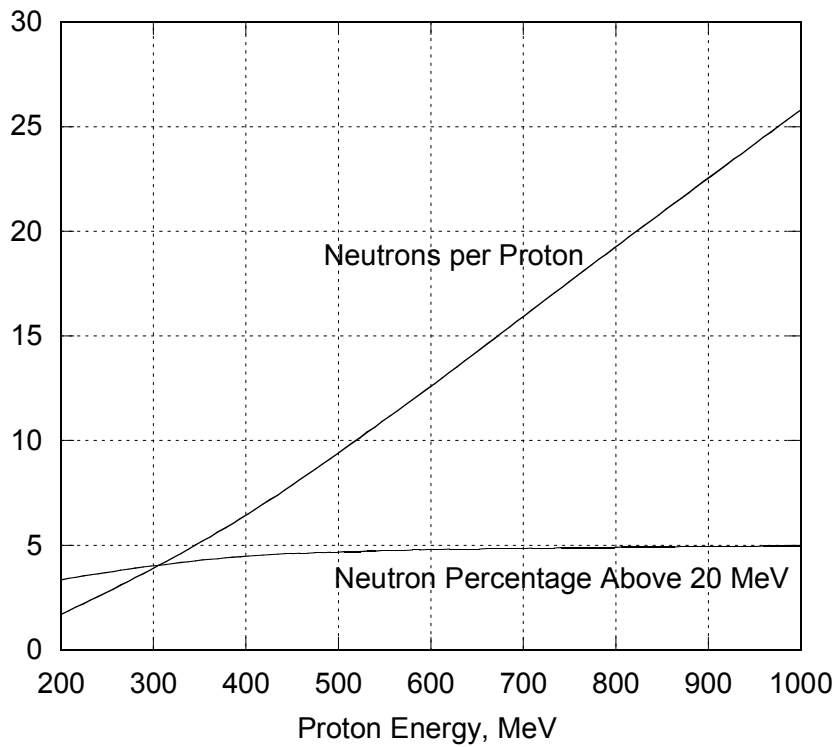


Figure 3. Number of neutrons per proton and neutron percentage with energy above 20 MeV as a function of the proton energy

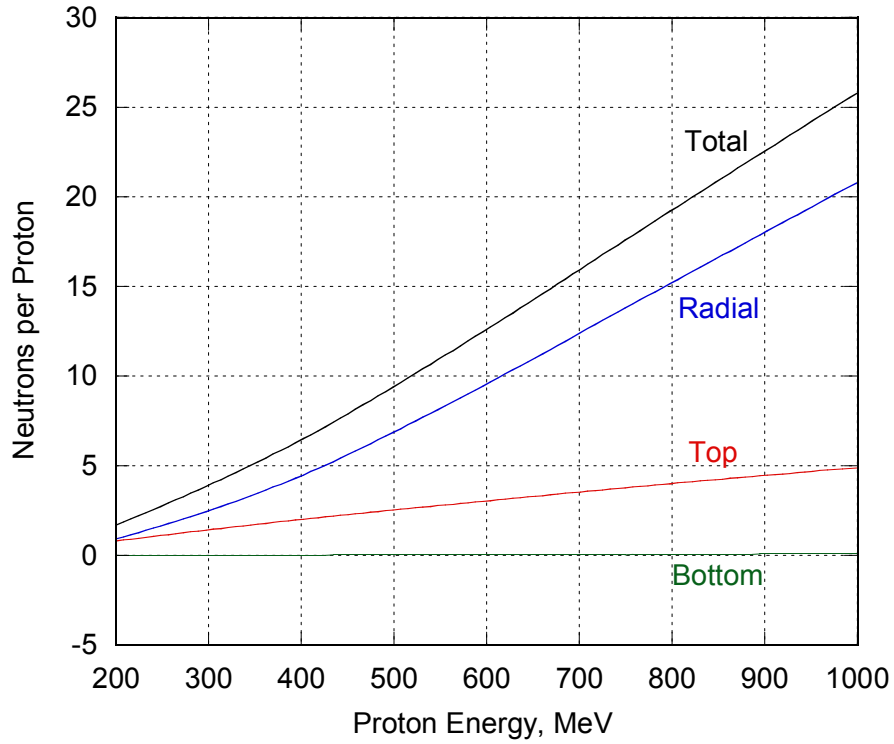


Figure 4. Neutron source spatial distribution at the target boundaries as a function of the proton energy

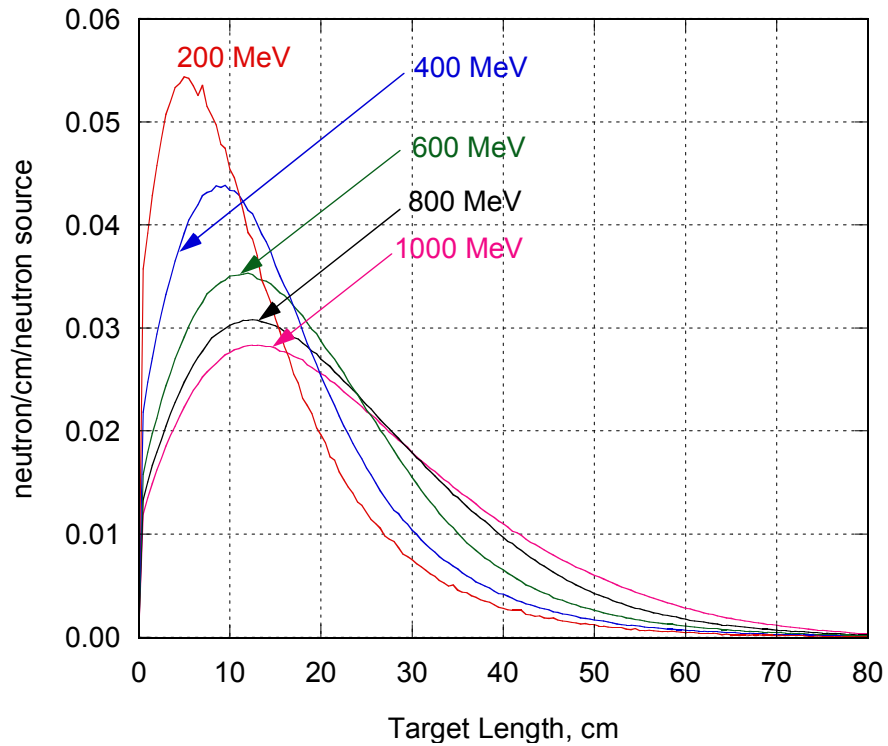


Figure 5. Neutron source distribution along the target buffer outer surface for different proton energies

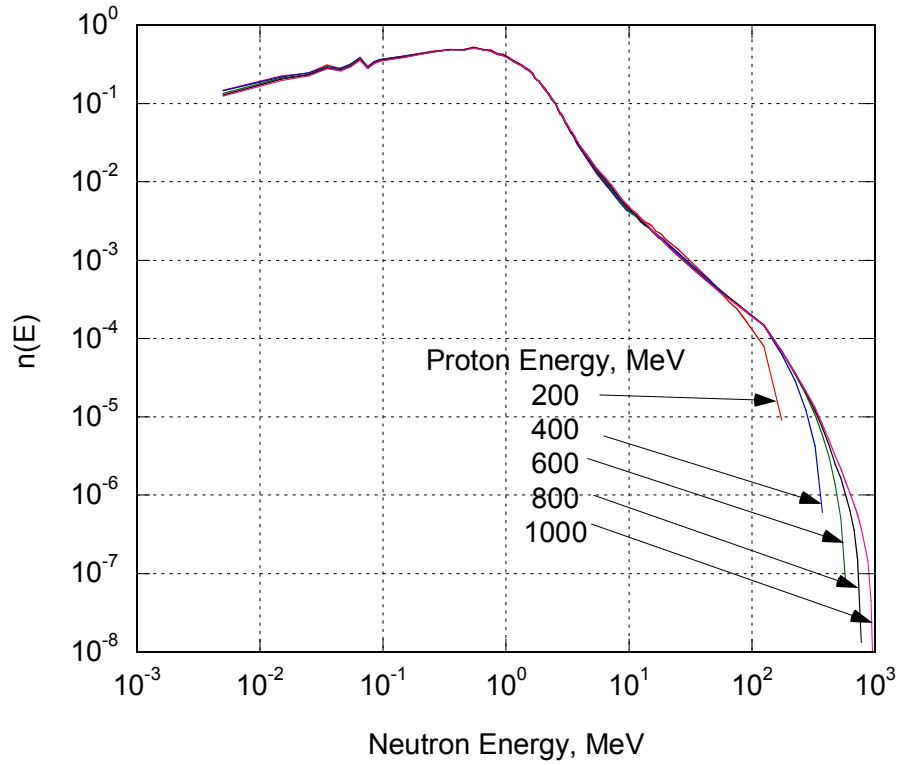


Figure 6. Neutron source spectrum for different proton energies

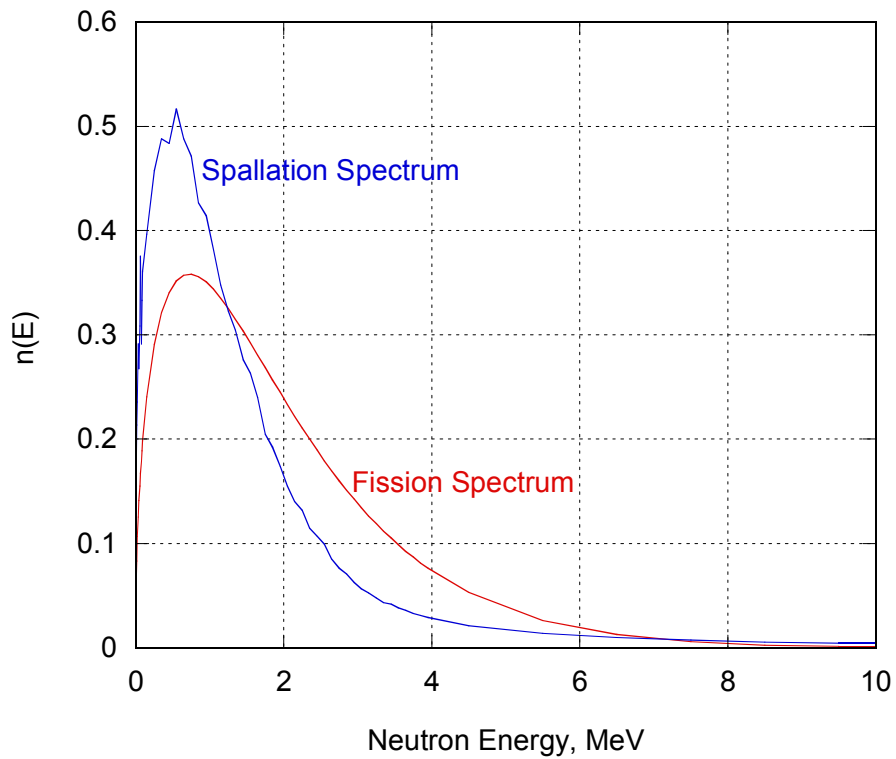


Figure 7. Fission spectrum compared to the spallation neutron source spectrum

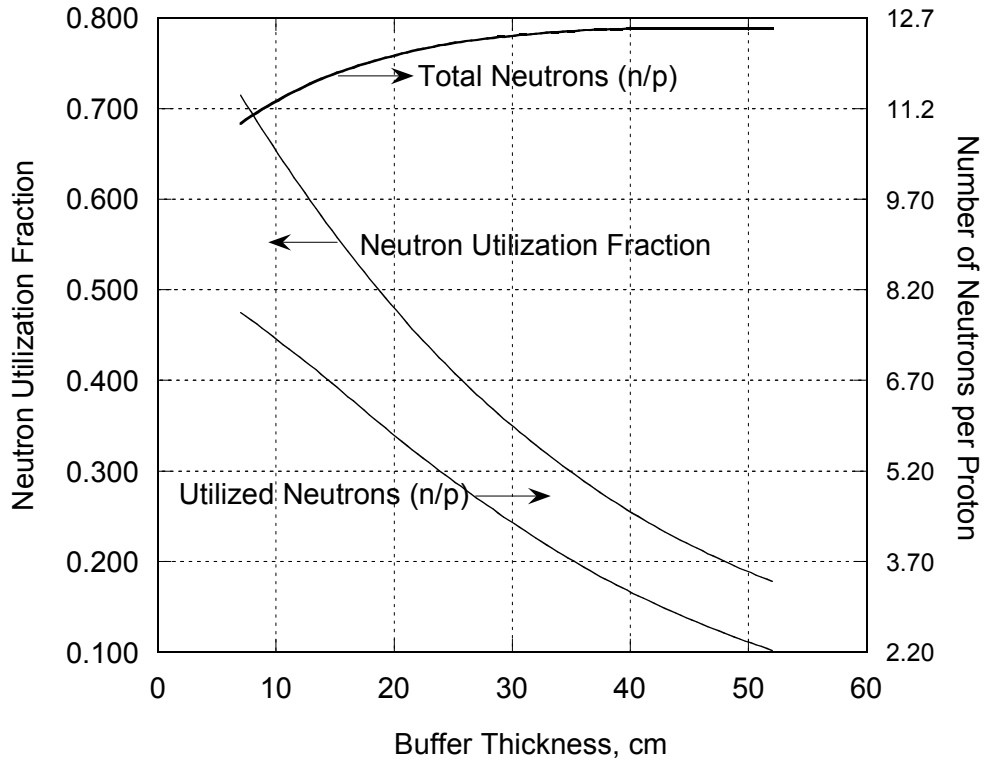


Figure 8. Neutron utilization and neutron yield as a function of the buffer size for 600 MeV proton beam

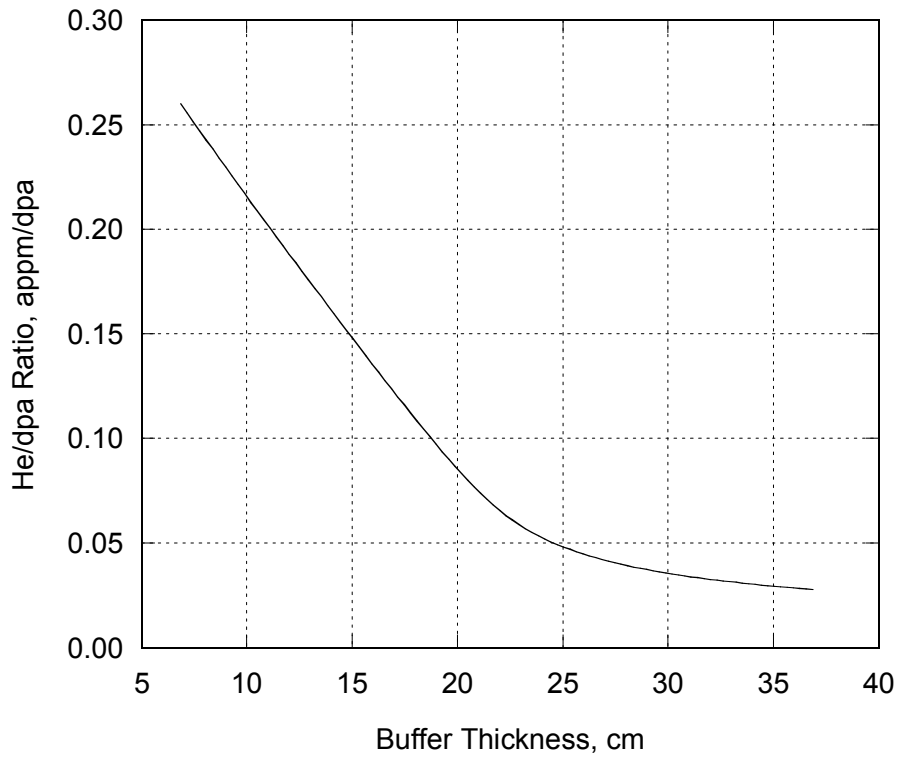


Figure 9. Transmuter structure helium/atomic displacement ratio as function of the buffer thickness for 600 MeV proton beam

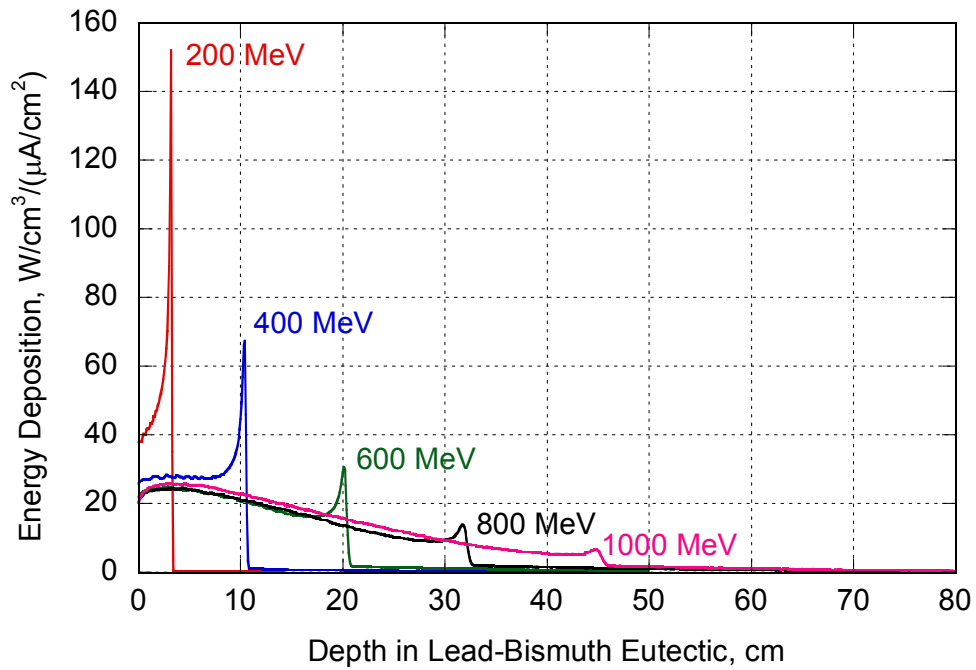


Figure 10. Spatial energy deposition in the lead-bismuth eutectic for different deuteron energies

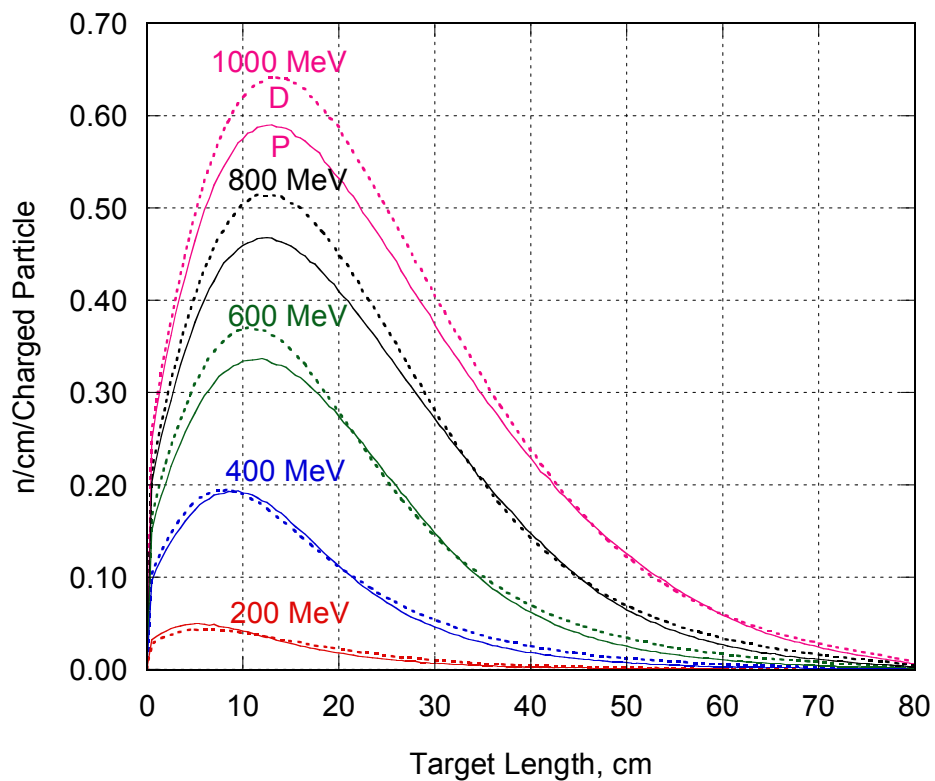


Figure 11. Neutron source distribution along the target buffer outer surface for different proton and deuteron energies

Table 1. Target window nuclear responses from 600 MeV proton beam with 40 $\mu\text{A}/\text{cm}^2$ current density

Energy deposition, W/cm^3	766.49
Atomic displacement, dpa/y	
Neutrons	46.2
Protons	21.1
Total	67.3
Helium production, appm/fpy	
Low energy neutrons ≤ 20 MeV	5.7
High energy neutrons > 20 MeV	50.2
Protons	1437.3
Total	1493.2
Hydrogen production, appm/fpy	
Low energy neutrons ≤ 20 MeV	6.3
High energy neutrons > 20 MeV	1010.1
Protons	26753.1
Total	27769.5